

Research Article

Bright Solitons in a \mathcal{PT} -Symmetric Chain of Dimers

Omar B. Kirikchi,¹ Alhaji A. Bachtiar,² and Hadi Susanto¹

¹Department of Mathematical Sciences, University of Essex, Wivenhoe Park, Colchester, Essex CO4 3SQ, UK

²Department of Mathematics, University of Indonesia, Depok, Indonesia

Correspondence should be addressed to Hadi Susanto; hsusanto@essex.ac.uk

Received 17 July 2016; Revised 17 September 2016; Accepted 17 October 2016

Academic Editor: Yao-Zhong Zhang

Copyright © 2016 Omar B. Kirikchi et al. This is an open access article distributed under the Creative Commons Attribution License, which permits unrestricted use, distribution, and reproduction in any medium, provided the original work is properly cited.

We study the existence and stability of fundamental bright discrete solitons in a parity-time- (\mathcal{PT} -) symmetric coupler composed by a chain of dimers that is modelled by linearly coupled discrete nonlinear Schrödinger equations with gain and loss terms. We use a perturbation theory for small coupling between the lattices to perform the analysis, which is then confirmed by numerical calculations. Such analysis is based on the concept of the so-called anticontinuum limit approach. We consider the fundamental onsite and intersite bright solitons. Each solution has symmetric and antisymmetric configurations between the arms. The stability of the solutions is then determined by solving the corresponding eigenvalue problem. We obtain that both symmetric and antisymmetric onsite mode can be stable for small coupling, in contrast to the reported continuum limit where the antisymmetric solutions are always unstable. The instability is either due to the internal modes crossing the origin or the appearance of a quartet of complex eigenvalues. In general, the gain-loss term can be considered parasitic as it reduces the stability region of the onsite solitons. Additionally, we analyse the dynamic behaviour of the onsite and intersite solitons when unstable, where typically it is either in the form of travelling solitons or soliton blow-ups.

1. Introduction

A system of equations is \mathcal{PT} -symmetric if it is invariant with respect to combined parity (\mathcal{P}) and time-reversal (\mathcal{T}) transformations. The symmetry is interesting as it forms a particular class of non-Hermitian Hamiltonians in quantum mechanics [1], which may have a real spectrum up to a critical value of the complex potential parameter, above which the system is in the “broken \mathcal{PT} symmetry” phase [2–4].

The most basic configuration having \mathcal{PT} symmetry is a dimer, that is, a system of two coupled oscillators where one of the oscillators has damping losses and the other one gains energy from external sources. Considerably, dimers are also the most important \mathcal{PT} systems as the concept of \mathcal{PT} symmetry was first realised experimentally on dimers consisting of two coupled optical waveguides [5, 6] (see also the review [7] for \mathcal{PT} symmetry in optical applications). The experiments have been rapidly followed by many other observations of \mathcal{PT} symmetry in different branches of physics, from mechanical to electrical analogues (see the review [8]).

When nonlinearity is present in a \mathcal{PT} system, one may have nontrivial behaviours that do not exist in the linear case, such as the presence of blow-up dynamics in the parameter region of the unbroken phase in the linear counterpart [9–11]. When nonlinear dimers are put in arrays where elements with gain and loss are linearly coupled to the elements of the same type belonging to adjacent dimers, one can also obtain a distinctive feature in the form of the existence of solutions localized in space as continuous families of their energy parameter [12]. The system therefore has two arms with each arm described by a discrete nonlinear Schrödinger equation with gain or loss. Here, we study the nonlinear localised solutions, which loosely we also refer to as bright discrete solitons, and their stability analytically and numerically.

In the continuous limit, the coupled equations without gain-loss have been studied in [13–16], where it has been shown that the system admits symmetric, antisymmetric, and asymmetric solitons between the arms. Unstable asymmetric solutions bifurcate from the symmetric ones through a subcritical symmetry breaking bifurcation, which then

become stable after a tangent (saddle-center) bifurcation. When one adds a gain and loss term in each arm, one obtains \mathcal{PT} -symmetric couplers, which have been considered in [17–22]. In the presence of the linear-gain and loss terms, asymmetric solitons cease to exist, while antisymmetric solitons are always unstable [20], even though those with small amplitudes can live long due to weak underlying instability [17]. Symmetric solitons can be stable in a similar fashion to those in the system without gain-loss [20].

The stability of bright discrete solitons in \mathcal{PT} -symmetric couplers was discussed in [12] using variational methods, where it was shown that symmetric onsite solutions can be stable and there is a critical solution amplitude above which the \mathcal{PT} symmetry is broken. The case when the polarity of the \mathcal{PT} -symmetric dimers is staggered along the chain is considered in [23]. The same equations without gain and loss were considered in [24] where the symmetric soliton loses its stability through the symmetry-breaking bifurcation at a finite value of the energy, similarly to that in the continuous counterpart [13–16]. Recently, a similar \mathcal{PT} chain of dimers with a slightly different nonlinearity was derived [25] to describe coupled chains of parametrically driven pendula as a mechanical analogue of \mathcal{PT} -symmetric systems [26]. The stability of bright discrete solitons was established through the applications of the Hamiltonian energy and an index theorem. The nonlinear long-time stability of the discrete solitons was also established using the Lyapunov method in the asymptotic limit of a weak coupling between the pendula [27].

In this work, we determine the eigenvalues of discrete solitons in \mathcal{PT} -symmetric couplers analytically using asymptotic expansions. The computation is based on the so-called method of weak coupling or anticontinuum limit. The application of the method in the study of discrete solitons was formulated rigorously in [28] for conservative systems. It was then applied to \mathcal{PT} -symmetric networks in [29, 30]. However, no explicit expression of the asymptotic series of the eigenvalues for the stability of discrete solitons has been presented before. Here, in addition to the asymptotic limit of weak coupling between the dimers, we also propose to consider expansions in the coefficient of the gain-loss terms. In this case, explicit computations of the asymptotic series of the eigenvalues become possible.

The manuscript is outlined as follows. In Section 2, we present the mathematical model. In Section 3, we use perturbation theory for small coupling to analyse the existence of fundamental localised solutions. Such analysis is based on the concept of the so-called anticontinuum limit approach. The stability of the solitons is then considered analytically in Section 4 by solving a corresponding eigenvalue problem. In this section, in addition to small coupling, the expansion is also performed under the assumption of small coefficient of the gain-loss term due to the nonsimple expression of the eigenvectors of the linearised operator. The findings obtained from the analytical calculations are then compared with the numerical counterparts in Section 5. We also produce stability regions for all the fundamental solitons numerically. In this section, we present the typical dynamics of solitons in the unstable parameter ranges by direct numerical integrations

of the governing equation. We present the conclusion in Section 6.

2. Mathematical Model

The governing equations describing \mathcal{PT} -symmetric chains of dimers are of the form [12]

$$\begin{aligned} \dot{u}_n &= i\sigma |u_n|^2 u_n + i\epsilon \Delta_2 u_n + \gamma u_n + i\nu_n, \\ \dot{v}_n &= i\sigma |v_n|^2 v_n + i\epsilon \Delta_2 v_n - \gamma v_n + iu_n. \end{aligned} \quad (1)$$

The derivative with respect to the evolution variable (i.e., the propagation distance, if we consider their application in fiber optics) is denoted by the overdot, $u_n = u_n(t)$ and $v_n = v_n(t)$ are complex-valued wave function at site $n \in \mathbb{Z}$, $\epsilon > 0$ is the constant coefficient of the horizontal linear coupling (coupling constant between two adjacent sites), $\Delta_2 u_n = (u_{n+1} - 2u_n + u_{n-1})$ and $\Delta_2 v_n = (v_{n+1} - 2v_n + v_{n-1})$ are the discrete Laplacian term in one spatial dimension, the gain and loss acting on complex variables u_n and v_n are represented by the positive coefficient γ ; that is, $\gamma > 0$. The nonlinearity coefficient is denoted by σ , which can be scaled to +1 without loss of generality due to the case of focusing nonlinearity that we consider. Bright discrete soliton solutions satisfy the localisation conditions $u_n, v_n \rightarrow 0$ as $n \rightarrow \pm\infty$.

The focusing system has static localised solutions that can be obtained from substituting

$$\begin{aligned} u_n &= A_n e^{i\omega t}, \\ v_n &= B_n e^{i\omega t} \end{aligned} \quad (2)$$

into (1) to yield the equations

$$\begin{aligned} \omega A_n &= |A_n|^2 A_n + \epsilon (A_{n+1} - 2A_n + A_{n-1}) - i\gamma A_n \\ &\quad + B_n, \\ \omega B_n &= |B_n|^2 B_n + \epsilon (B_{n+1} - 2B_n + B_{n-1}) + i\gamma B_n + A_n, \end{aligned} \quad (3)$$

where A_n and B_n are complex-valued and the propagation constant $\omega \in \mathbb{R}$.

3. Solutions of Weakly Coupled Equations

In the uncoupled limit, that is, when $\epsilon = 0$, chain (1) becomes the equations for the dimer. The static equation (3) has been analysed in detail in [29, 31], where it was shown that there is a relation between ω and γ above which there is no time-independent solution to (3) (see also the analysis below). When ϵ is nonzero, but small enough, the existence of solutions emanating from the uncoupled limit can be shown using the Implicit Function Theorem. The existence analysis of [25] can be adopted here despite the slightly different nonlinearity as the Jacobian of our system when uncoupled shares a rather similar invertible structure (see also [29, 30] that have the same nonlinearity in the governing equations but different small coupling terms). However, below we will

not state the theorem and instead derive the asymptotic series of the solutions.

Using perturbation expansion, solutions of the coupler (3) for small coupling constant ϵ can be expressed analytically as

$$\begin{aligned} A_n &= A_n^{(0)} + \epsilon A_n^{(1)} + \dots, \\ B_n &= B_n^{(0)} + \epsilon B_n^{(1)} + \dots. \end{aligned} \quad (4)$$

By substituting the above expansions into (3) and collecting the terms in successive powers of ϵ , one obtains at $\mathcal{O}(1)$ and $\mathcal{O}(\epsilon)$, respectively, the equations

$$\begin{aligned} A_n^{(0)} &= B_n^{(0)} (\omega - B_n^{(0)} B_n^{*(0)} - i\gamma), \\ B_n^{(0)} &= A_n^{(0)} (\omega - A_n^{(0)} A_n^{*(0)} + i\gamma), \\ A_n^{(1)} &= B_n^{(1)} (\omega - 2B_n^{(0)} B_n^{*(0)} - i\gamma) - B_n^{(0)2} B_n^{*(1)} - \Delta_2 B_n^{(0)}, \\ B_n^{(1)} &= A_n^{(1)} (\omega - 2A_n^{(0)} A_n^{*(0)} + i\gamma) - A_n^{(0)2} A_n^{*(1)} \\ &\quad - \Delta_2 A_n^{(0)}. \end{aligned} \quad (5)$$

It is well-known that there are two natural fundamental solutions representing bright discrete solitons that may exist for any ϵ , from the anticontinuum to the continuum limit, that is, an intersite (two-excited-site) and onsite (one-excited-site) bright discrete mode. Here, we will limit our study to these two fundamental modes.

3.1. Intersite Soliton. In the uncoupled limit, the mode structures $A_n^{(0)}$ and $B_n^{(0)}$ for the intersite soliton are of the form

$$\begin{aligned} A_n^{(0)} &= \begin{cases} \widehat{a}_0 e^{i\phi_a} & n = 0, 1, \\ 0 & \text{otherwise,} \end{cases} \\ B_n^{(0)} &= \begin{cases} \widehat{b}_0 e^{i\phi_b} & n = 0, 1, \\ 0 & \text{otherwise,} \end{cases} \end{aligned} \quad (7)$$

with [31]

$$\widehat{a}_0 = \widehat{b}_0 = \sqrt{\omega \mp \sqrt{1 - \gamma^2}}, \quad (8)$$

$$\sin(\phi_b - \phi_a) = \gamma,$$

which is an exact solution of (5). Note that (8) will have no real solution when $|\gamma| > 1$. This is the broken region of \mathcal{PT} -symmetry. The parameter ϕ_a can be taken as 0, due to the gauge phase invariance of the governing equation (1) and henceforth $\phi_b = \arcsin \gamma$ and $\pi - \arcsin \gamma$. The former phase corresponds to the so-called symmetric configuration between the arms, while the latter is called antisymmetric one. Herein, we also refer to the symmetric and antisymmetric soliton as soliton I and II, respectively. Equation (8) informs us that $\omega > \sqrt{1 - \gamma^2} > 0$ and $\omega > -\sqrt{1 - \gamma^2}$ are the necessary conditions for solitons I and II, respectively.

For the first-order correction due to the weak coupling, writing $A_n^{(1)} = \widetilde{a}_{n,1} e^{i\phi_a}$ and $B_n^{(1)} = \widetilde{b}_{n,1} e^{i\phi_b}$ and substituting them into (6) will yield

$$\widetilde{a}_{n,1} = \widetilde{b}_{n,1} = \begin{cases} \frac{1}{(2\widehat{a}_0)} & n = 0, 1, \\ \frac{1}{\widehat{a}_0} & n = -1, 2, \\ 0 & \text{otherwise.} \end{cases} \quad (9)$$

Equations (4), (7), (8), and (9) are the asymptotic expansion of the intersite solitons. One can continue the same calculation to obtain higher order corrections. Here, we limit ourselves to the first-order correction only, which is sufficient to determine the leading order behaviour of the eigenvalues later.

3.2. Onsite Soliton. For the onsite soliton, that is, a one-excited-site discrete mode, one can perform the same computations to obtain the mode structure of the form

$$\begin{aligned} A_n^{(0)} &= \begin{cases} \widehat{a}_0 e^{i\phi_a} & n = 0, \\ 0 & \text{otherwise,} \end{cases} \\ B_n^{(0)} &= \begin{cases} \widehat{b}_0 e^{i\phi_b} & n = 0, \\ 0 & \text{otherwise,} \end{cases} \end{aligned} \quad (10)$$

with (8). After writing $A_n^{(1)} = \widetilde{a}_{n,1} e^{i\phi_a}$ and $B_n^{(1)} = \widetilde{b}_{n,1} e^{i\phi_b}$, the first order correction from (6) is given by

$$\widetilde{a}_{n,1} = \widetilde{b}_{n,1} = \begin{cases} \frac{1}{\widehat{a}_0} & n = 0, \pm 1, \\ 0 & \text{otherwise.} \end{cases} \quad (11)$$

4. Stability Analysis

After we find discrete solitons, their linear stability is then determined by solving a corresponding linear eigenvalue problem. To do so, we introduce the linearisation ansatz $u_n = (A_n + \widetilde{\epsilon}(K_n + iL_n)e^{\lambda t})e^{i\omega t}$ and $v_n = (B_n + \widetilde{\epsilon}(P_n + iQ_n)e^{\lambda t})e^{i\omega t}$, $|\widetilde{\epsilon}| \ll 1$, and substitute this into (1) to obtain the linearised equations at $\mathcal{O}(\widetilde{\epsilon})$:

$$\begin{aligned} \lambda K_n &= -(A_n^2 - \omega)L_n - \epsilon(L_{n+1} - 2L_n + L_{n-1}) + \gamma K_n \\ &\quad - Q_n, \end{aligned}$$

$$\lambda L_n = (3A_n^2 - \omega) K_n + \epsilon (K_{n+1} - 2K_n + K_{n-1}) + \gamma L_n + P_n,$$

$$\begin{aligned} \lambda P_n &= -(\Re(B_n)^2 + 3\Im(B_n)^2 - \omega) Q_n \\ &\quad - \epsilon (Q_{n+1} - 2Q_n + Q_{n-1}) \\ &\quad - (2\Re(B_n)\Im(B_n) + \gamma) P_n - L_n, \end{aligned}$$

$$\begin{aligned} \lambda Q_n &= (3\Re(B_n)^2 + \Im(B_n)^2 - \omega) P_n \\ &\quad + \epsilon (P_{n+1} - 2P_n + P_{n-1}) \\ &\quad + (2\Re(B_n)\Im(B_n) - \gamma) Q_n + K_n, \end{aligned} \quad (12)$$

which have to be solved for the eigenvalue λ and the corresponding eigenvector $[\{K_n\}, \{L_n\}, \{P_n\}, \{Q_n\}]^T$. As the stability matrix of the eigenvalue problem (12) is real valued, $\bar{\lambda}$ and $-\lambda$ are also eigenvalues with corresponding eigenvectors $[\{\bar{K}_n\}, \{\bar{L}_n\}, \{\bar{P}_n\}, \{\bar{Q}_n\}]^T$ and $[\{K_n\}, \{-L_n\}, \{P_n\}, \{-Q_n\}]^T$ with $\gamma \rightarrow -\gamma$, respectively. Therefore, we can conclude that the solution u_n is (linearly) stable only when $\Re(\lambda) = 0$ for all eigenvalues λ .

4.1. Continuous Spectrum. The spectrum of (12) will consist of continuous spectrum and discrete spectrum (eigenvalue). To investigate the former, we consider the limit $n \rightarrow \pm\infty$, introduce the plane-wave ansatz $K_n = \hat{k}e^{ik_n}$, $L_n = \hat{l}e^{ik_n}$, $P_n = \hat{p}e^{ik_n}$, and $Q_n = \hat{q}e^{ik_n}$, $k \in \mathbb{R}$, and substitute the ansatz into (12) to obtain

$$\lambda \begin{bmatrix} \hat{k} \\ \hat{l} \\ \hat{p} \\ \hat{q} \end{bmatrix} = \begin{bmatrix} \gamma & \xi & 0 & -1 \\ -\xi & \gamma & 1 & 0 \\ 0 & -1 & -\gamma & \xi \\ 1 & 0 & -\xi & -\gamma \end{bmatrix} \begin{bmatrix} \hat{k} \\ \hat{l} \\ \hat{p} \\ \hat{q} \end{bmatrix}, \quad (13)$$

where $\xi = \omega - 2\epsilon(\cos k - 1)$. The equation can be solved analytically to yield the dispersion relation

$$\begin{aligned} \lambda^2 &= 4\epsilon\omega(\cos k - 1) - 4\epsilon^2(\cos k - 1)^2 - \omega^2 - 1 + \gamma^2 \\ &\quad \pm (4\epsilon(\cos k - 1) - 2\omega)\sqrt{1 - \gamma^2}. \end{aligned} \quad (14)$$

The continuous spectrum is therefore given by $\lambda \in \pm[\lambda_{1-}, \lambda_{2-}]$ and $\lambda \in \pm[\lambda_{1+}, \lambda_{2+}]$ with the spectrum boundaries

$$\begin{aligned} \lambda_{1\pm} &= i\sqrt{1 - \gamma^2 + \omega^2 \pm 2\omega\sqrt{1 - \gamma^2}}, \\ \lambda_{2\pm} &= i\sqrt{1 - \gamma^2 + 8\epsilon\omega + 16\epsilon^2 + \omega^2 + 2\sqrt{1 - \gamma^2}(\pm\omega - 4\epsilon)}, \end{aligned} \quad (15)$$

obtained from (14) by setting $k = 0$ and $k = \pi$ in the equation.

4.2. Discrete Spectrum. Following the weak-coupling analysis as in Section 3, we will as well use similar asymptotic expansions to solve the eigenvalue problem (12) analytically; that is, we write

$$\square = \square^{(0)} + \sqrt{\epsilon}\square^{(1)} + \epsilon\square^{(2)} + \dots, \quad (16)$$

with $\square = \lambda, K_n, L_n, P_n, Q_n$. We then substitute the expansions into the eigenvalue problem (12).

At order $\mathcal{O}(1)$, one will obtain the stability equation for the dimer, which has been discussed for a general value of γ in [31]. The expression of the eigenvalues is simple, but the expression of the corresponding eigenvectors is not, which makes the result of [31] rather impractical to use. Therefore, here we limit ourselves to the case of small $|\gamma|$ and expand (16) further as

$$\square^{(j)} = \square^{(j,0)} + \gamma\square^{(j,1)} + \gamma^2\square^{(j,2)} + \dots, \quad (17)$$

$j = 0, 1, 2, \dots$. Hence, we have two small parameters, that is, ϵ and γ , that are independent of each other. For the sake of presentation, the detailed calculations are shown in the Appendix. Here we will only cite the final results.

4.2.1. Intersite Soliton I. The intersite soliton I (i.e., the symmetric intersite soliton) has three pairs of eigenvalues for small ϵ and γ . One pair bifurcate from the zero eigenvalue. They are asymptotically given by

$$\begin{aligned} \lambda &= \sqrt{\epsilon} \left(2\sqrt{\omega - 1} + \frac{\gamma^2}{(2\sqrt{\omega - 1})} + \dots \right) + \mathcal{O}(\epsilon), \\ \lambda &= \begin{cases} \left(2\sqrt{\omega - 2} - \gamma^2 \frac{\omega - 4}{2\sqrt{\omega - 2}} + \dots \right) + \epsilon \left(\sqrt{\omega - 2} - \gamma^2 \frac{\omega}{4\sqrt{\omega - 2}} + \dots \right) + \mathcal{O}(\epsilon)^{3/2}, \\ \left(2\sqrt{\omega - 2} - \gamma^2 \frac{\omega - 4}{2\sqrt{\omega - 2}} + \dots \right) + \epsilon \left(\frac{1}{\sqrt{\omega - 2}} - \gamma^2 \frac{\omega}{4(\omega - 2)^{3/2}} + \dots \right) + \mathcal{O}(\epsilon)^{3/2}. \end{cases} \end{aligned} \quad (18)$$

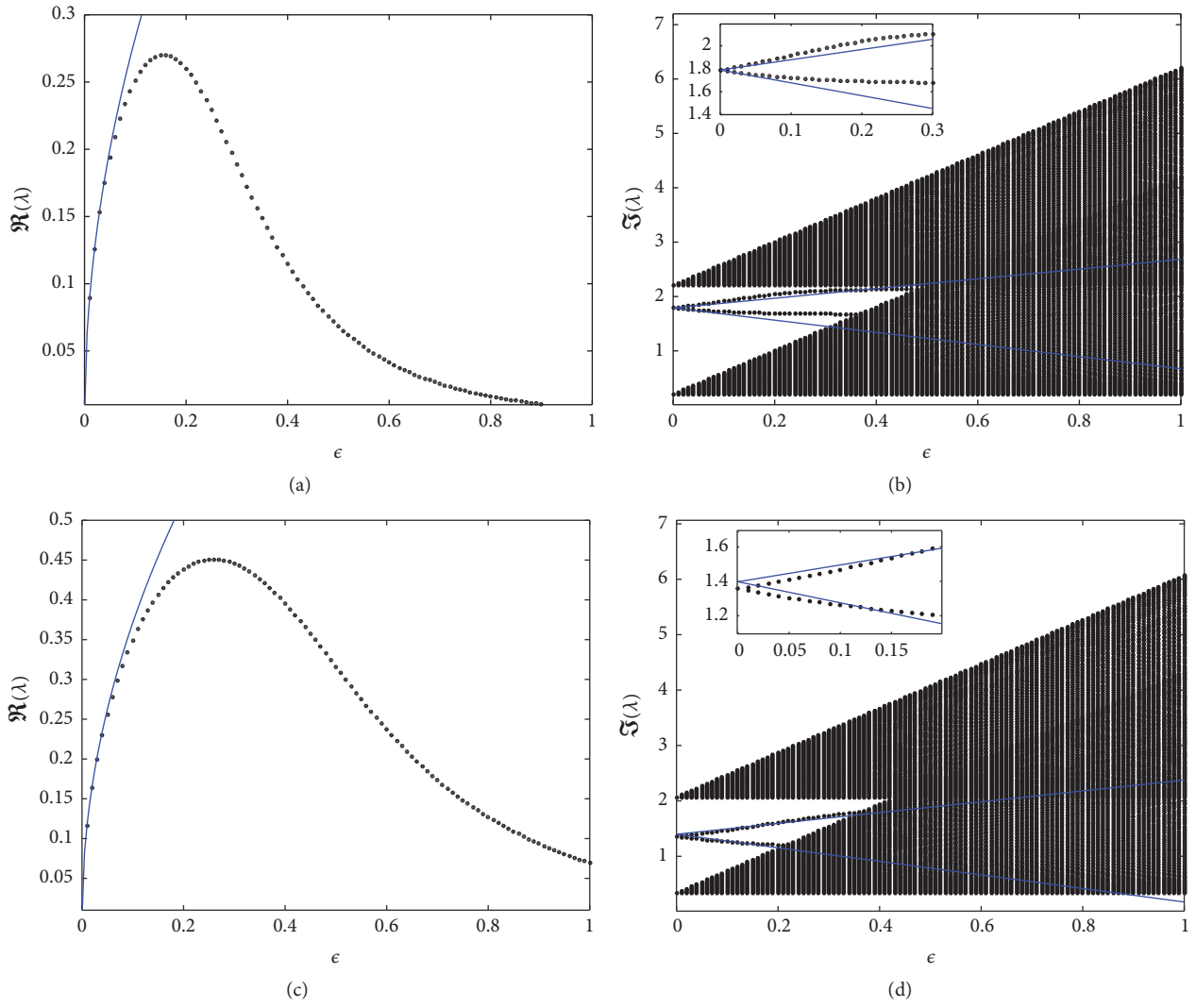


FIGURE 1: Eigenvalues of intersite soliton I with $\omega = 1.2, \gamma = 0$ (a, b) and 0.5 (c, d). Dots are from the numerics and solid lines are the asymptotic approximations in Section 4.2.1. The collection of dots forming black regions in the right column corresponds to the continuous spectrum.

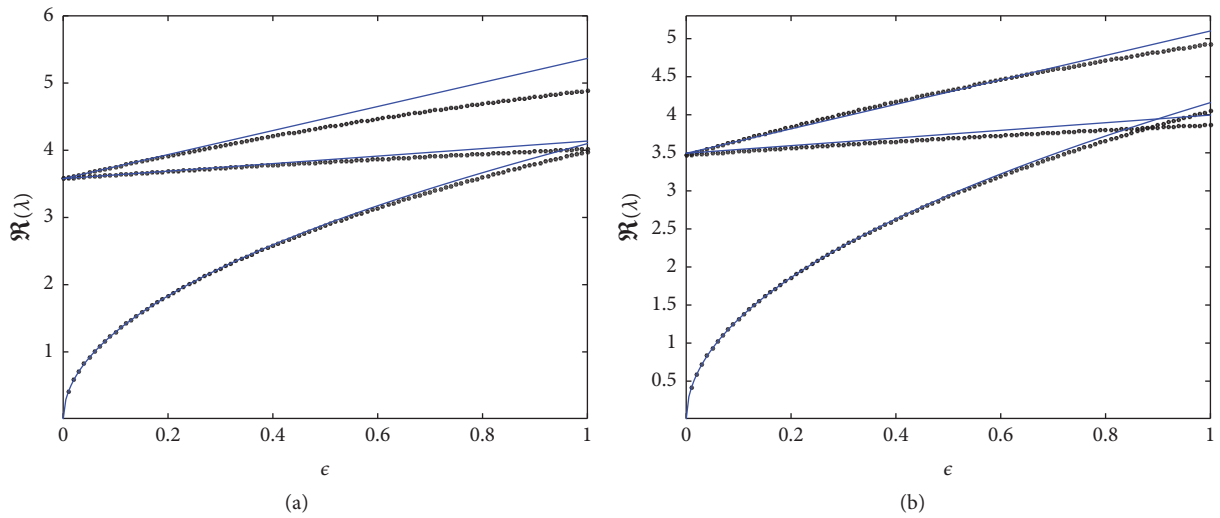


FIGURE 2: The same as in Figure 1 with $\gamma = 0$ (a) and $\gamma = 0.5$ (b), but for $\omega = 5.2$. In this case, all the eigenvalues are real.

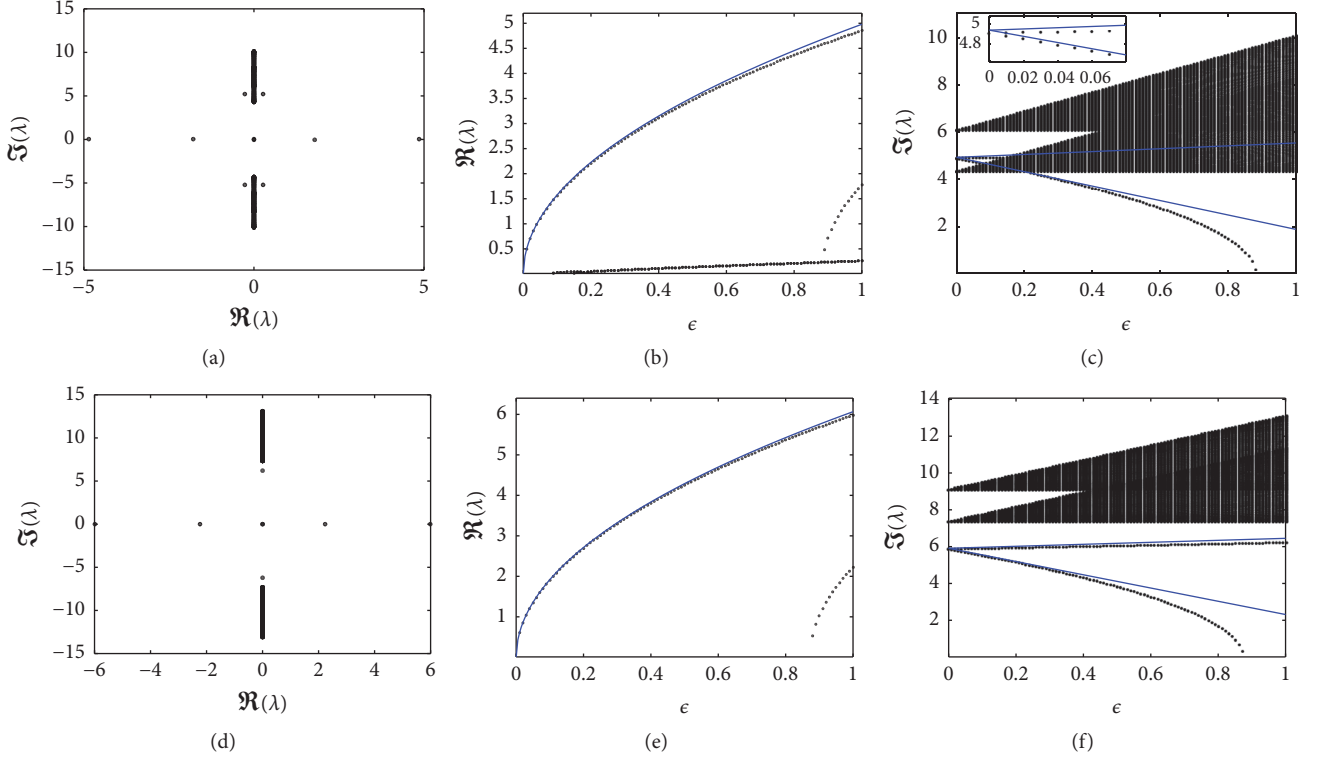


FIGURE 3: The spectra of intersite soliton II with $\omega = 5.2$ (a, b, c) and 8.2 (d, e, f) and $\gamma = 0.5$. The most left panels are the spectra in the complex plane for $\epsilon = 1$. (b, c, e, f) The eigenvalues as a function the coupling constant. Solid blue curves are the asymptotic approximations.

4.2.2. *Intersite Soliton II.* The intersite soliton II, that is, the intersite soliton that is antisymmetric between the arms, has three pairs of eigenvalues given by

$$\lambda = \sqrt{\epsilon} \left(2\sqrt{\omega+1} - \frac{\gamma^2}{(2\sqrt{\omega+1})} + \dots \right) + \mathcal{O}(\epsilon),$$

$$\lambda = \begin{cases} i \left(2\sqrt{\omega+2} - \gamma^2 \frac{\omega+4}{2\sqrt{\omega+2}} + \dots \right) - i\epsilon \left(\sqrt{\omega+2} + \gamma^2 \frac{3\omega^4 + 35\omega^3 + 136\omega^2 + 208\omega + 108}{8\sqrt{\omega+2}(\omega^3 + 6\omega^2 + 12\omega + 8)} + \dots \right) + \mathcal{O}(\epsilon)^{3/2}, \\ i \left(2\sqrt{\omega+2} - \gamma^2 \frac{\omega+4}{2\sqrt{\omega+2}} + \dots \right) + i\epsilon \left(\frac{1}{\sqrt{\omega+2}} + \gamma^2 \frac{\omega^4 + 21\omega^3 + 104\omega^2 + 184\omega + 108}{8\sqrt{\omega+2}(\omega^3 + 6\omega^2 + 12\omega + 8)} + \dots \right) + \mathcal{O}(\epsilon)^{3/2}. \end{cases} \quad (19)$$

4.2.3. *Onsite Soliton I.* The onsite soliton has only one eigenvalue for small ϵ given asymptotically by

$$\lambda = \left(2\sqrt{\omega-2} - \gamma^2 \frac{\omega-4}{2\sqrt{\omega-2}} + \dots \right) + \epsilon \left(\frac{2}{\sqrt{\omega-2}} - \gamma^2 \frac{\omega}{2(\omega-2)^{3/2}} + \dots \right) + \dots. \quad (20)$$

4.3. *Onsite Soliton II.* As for the second type of the onsite soliton, we have

$$\lambda = i \left(2\sqrt{\omega+2} - \gamma^2 \frac{\omega+4}{\sqrt{\omega+2}} + \dots \right) + 2i\epsilon \left(\frac{1}{\sqrt{\omega+2}} - \gamma^2 \frac{\omega}{(\omega+2)^{3/2}} + \dots \right) + \dots. \quad (21)$$

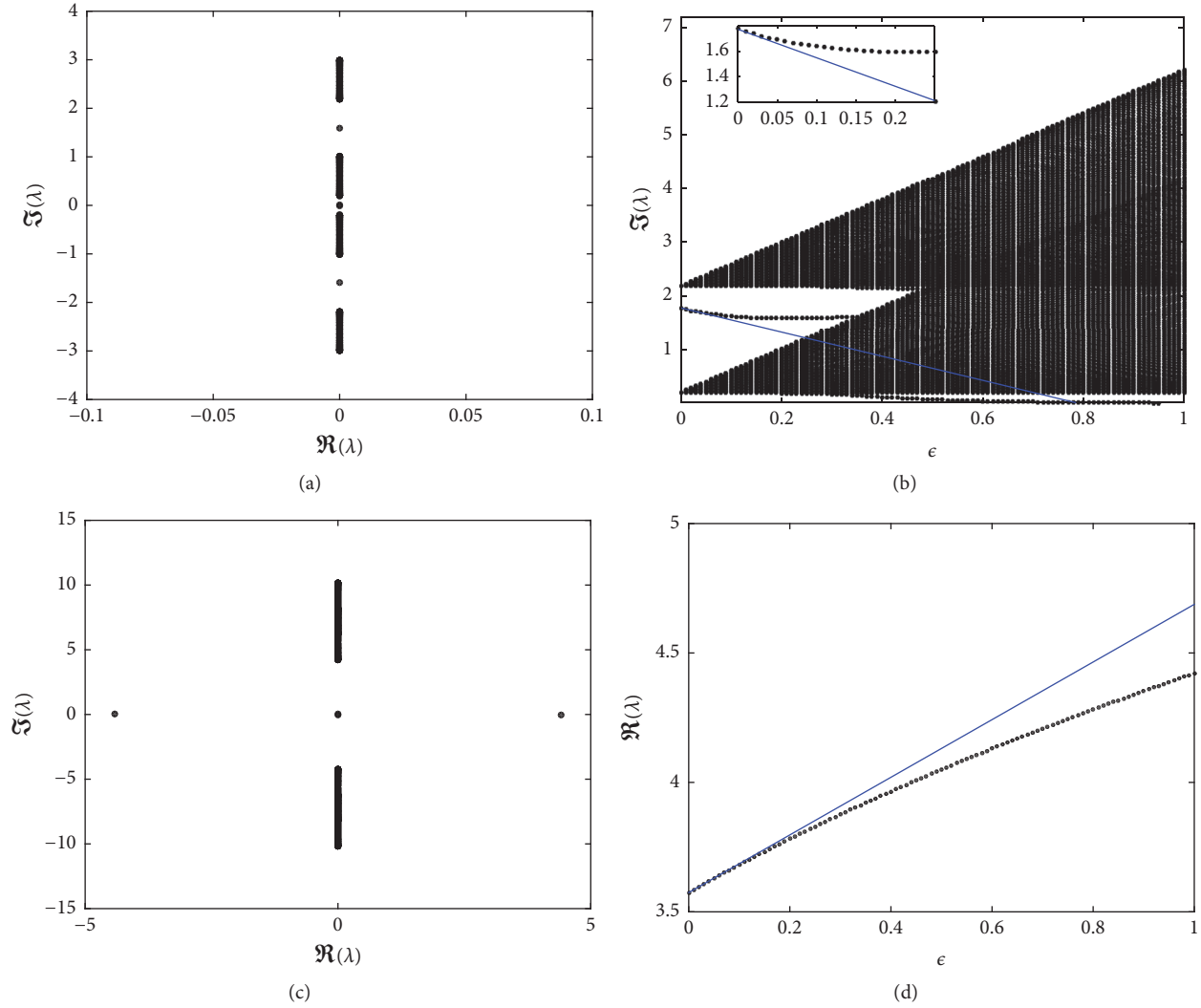


FIGURE 4: (a, c) The spectrum of onsite soliton I in the complex plane for $\epsilon = 0.2$. (b, d) The eigenvalue as a function of the coupling and its approximation from Section 4.2.3. (a–d) are for $\omega = 1.2$ and 5.2 , respectively. Here, $\gamma = 0.1$.

5. Numerical Results

We have solved the steady-state equation (3) numerically using a Newton-Raphson method and analysed the stability of the numerical solution by solving the eigenvalue problem (12). Here we will compare the analytical calculations obtained above with the numerical results.

First, we consider the discrete intersite soliton I. We show in Figure 1 the spectrum of the soliton as a function of the coupling constant ϵ for $\omega = 1.2$ and $\gamma = 0, 0.5$. On the real axis, one can observe that there is only one unstable eigenvalue that bifurcates from the origin. As the coupling increases, the bifurcating eigenvalue enters the origin again when $\epsilon \rightarrow \infty$. Hence, in that limit we obtain a stable soliton I (i.e., a stable symmetric soliton). The dynamics of the nonzero eigenvalues as a function of the coupling constant is shown in the right panels of the figure, where one can see that the eigenvalues are on the imaginary axis and simply enter the continuous spectrum as ϵ increases.

In Figure 2, we plot the eigenvalues for ω large enough. Here, in the uncoupled limit, all the three pairs of eigenvalues are on the real axis. As the coupling increases, two pairs go back toward the origin, while one pair remains on the real axis (not shown here). In the continuum limit $\epsilon \rightarrow \infty$, we therefore obtain an unstable soliton I (i.e., an unstable symmetric soliton).

In both figures, we also plot the approximate eigenvalues in solid (blue) curves, where good agreement is obtained for small ϵ .

From numerical computations, we conjecture that if in the limit $\epsilon \rightarrow 0$ all the nonzero eigenvalues λ satisfy $\lambda^2 > \lambda_{1-}^2$ (see (15)), then we will obtain unstable soliton I in the continuum limit $\epsilon \rightarrow \infty$. However, when in the anticontinuum limit $\epsilon \rightarrow 0$ all the nonzero eigenvalues λ satisfy $\lambda_{1+}^2 < \lambda^2 < \lambda_{2-}^2$, we may either obtain a stable or an unstable soliton I in the continuum limit.

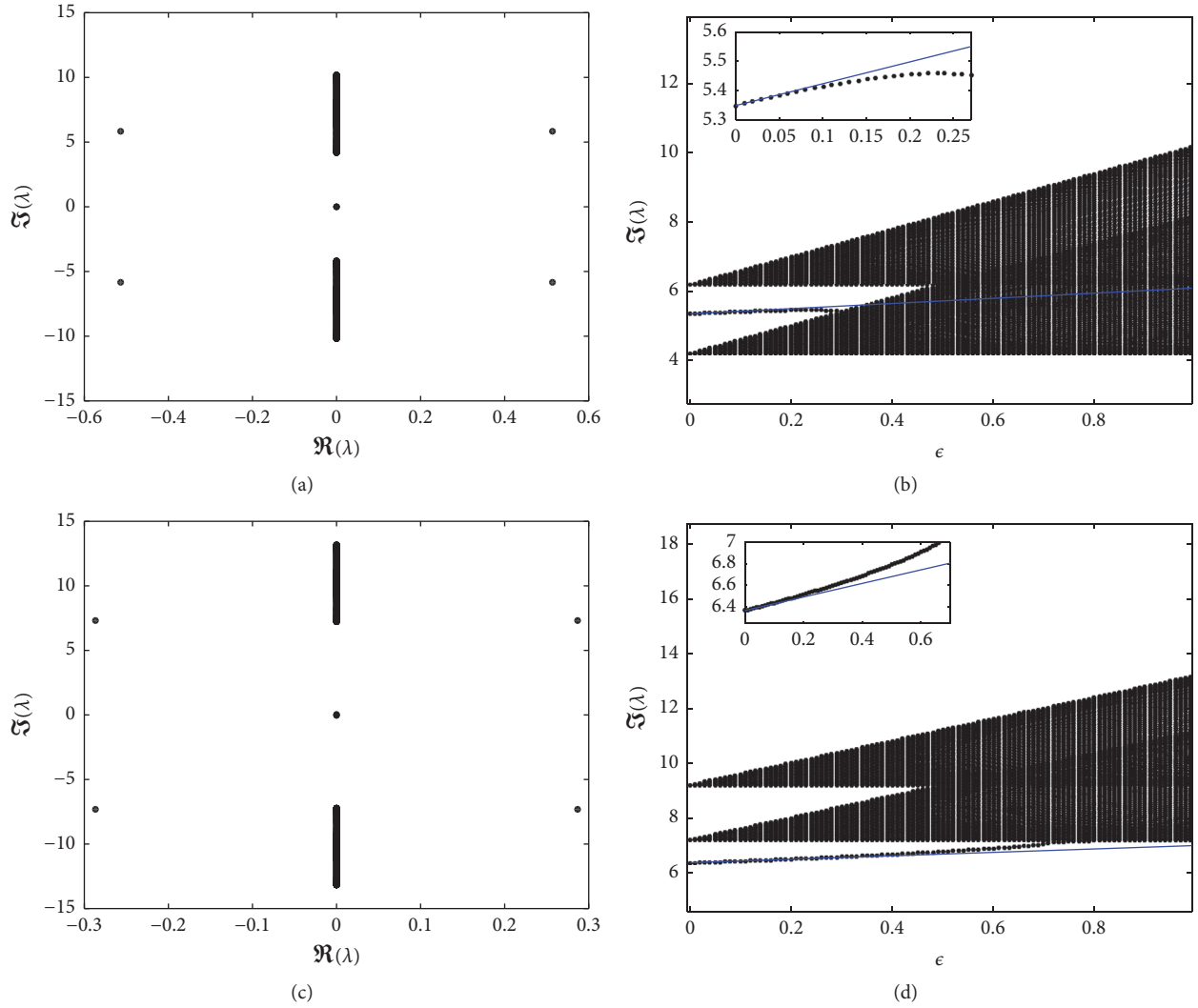


FIGURE 5: The same as in Figure 4, but for onsite soliton II with $\omega = 5.2$ (a, b) and 8.2 (c, d). (a, c) are with $\epsilon = 1$.

Next, we consider intersite solitons II (i.e., antisymmetric intersite solitons). Shown in Figure 3 is the spectrum of the discrete solitons for two values of ω . In both cases, there is an eigenvalue bifurcating from the origin. For the smaller value of ω (Figures 3(a)–3(c)), we have the condition that all the nonzero eigenvalues λ satisfy $\lambda^2 < \lambda_{2-}^2$ in the anti-continuum limit $\epsilon \rightarrow 0$. The collision between the eigenvalues and the continuous spectrum as the coupling increases creates complex eigenvalues. In the second case using larger ω (Figures 3(d)–3(f)), the nonzero eigenvalues λ satisfy $\lambda^2 > \lambda_{1-}^2$ when $\epsilon = 0$. Even though not seen in the figure, the collision between one of the nonzero eigenvalues and the continuous spectrum also creates a pair of complex eigenvalues. Additionally, in the continuum limit both values of ω as well as the other values of the parameter that we computed for this type of discrete solitons yield unstable solutions.

We also study onsite solitons. Shown in Figures 4 and 5 is the stability of discrete solitons types I and II, respectively.

Figure 4(a) shows that for $(\omega - \sqrt{1 - \gamma^2})$ small enough we will obtain stable discrete solitons. For coupling constant ϵ

small, we indeed show it through our analysis depicted as the blue solid line. Numerically, we obtain that this soliton is also stable in the continuum limit $\epsilon \rightarrow \infty$. However, when ω is large enough compared to $\sqrt{1 - \gamma^2}$, even though initially in the uncoupled limit the nonzero eigenvalue λ satisfies $\lambda^2 < \lambda_{2-}^2$, one may obtain an exponential instability (i.e., instability due to a real eigenvalue). Figure 4(c) shows the case when the discrete soliton is already unstable even in the uncoupled limit due to the nonzero eigenvalue that is already real-valued.

Figure 5 shows that the antisymmetric solitons are generally unstable due to a quartet of complex eigenvalues, as shown in Figures 5(a) and 5(c). When the coupling is increased further, there will be an eigenvalue bifurcating from $\pm\lambda_{1-}$ that will move towards the origin and later becomes a pair of real eigenvalues. These solitons are also unstable in the continuum limit.

Unlike intersite discrete solitons that are always unstable, onsite discrete solitons may be stable. In Figure 6, we present the (in)stability region of the two types of discrete solitons in the (ϵ, ω) -plane for three values of the gain-loss parameter γ .

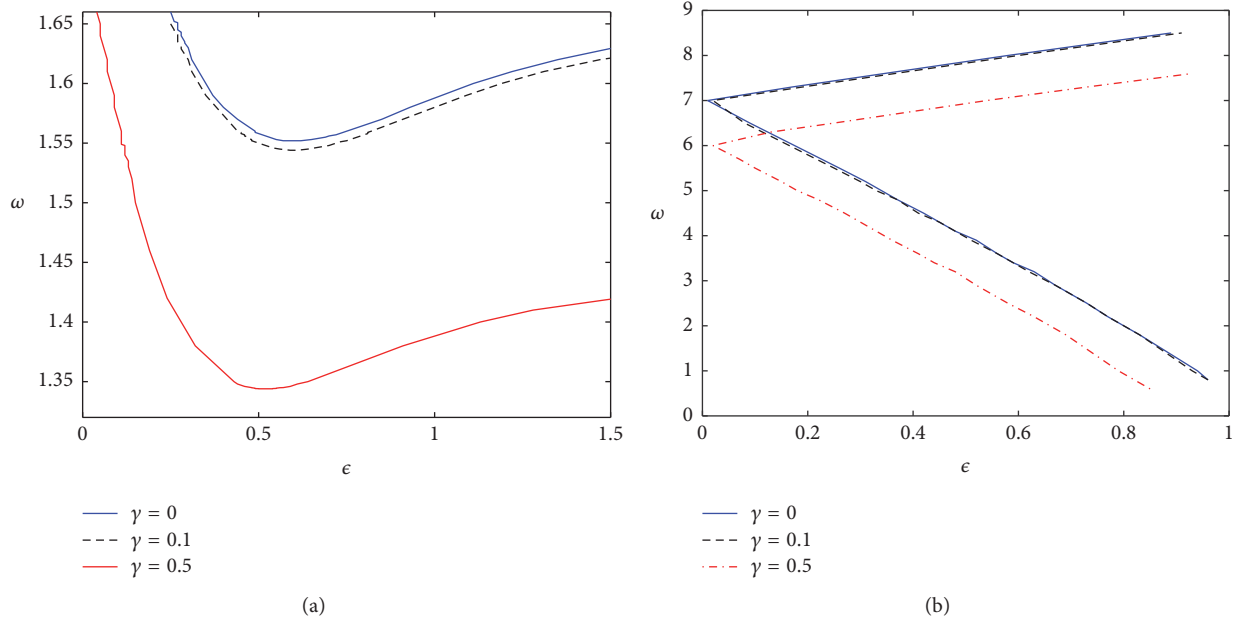


FIGURE 6: The stability region of the onsite soliton type I (a) and II (b) in the (ϵ, ω) -plane for several values of γ . The solutions are unstable above the curves in panel (a) and between the curves in panel (b).

Discrete solitons are unstable above the curves in panel (a) and between the curves in panel (b). Indeed as we mentioned before, for soliton I there is a critical ω that depends on γ below which the soliton is stable in the continuum limit, while soliton II is always unstable in that limit. Another difference between the two figures is that the stability curves in Figure 6(a) generally correspond to an eigenvalue crossing the origin that becomes real-valued, while the curves in the other panel are due to the appearance of a quartet of complex eigenvalues. In general, we obtain that the gain-loss term can be parasitic as it reduces the stability region of the discrete solitons.

Finally, we present in Figure 7 the time dynamics of some of the unstable solutions shown in the previous figures. What we obtain is that typically there are two kinds of dynamics, that is, in the form of travelling discrete solitons or solution blow-ups. The first type was the typical dynamics of the intersite soliton I. The second dynamics is typical for the other types of unstable discrete solitons.

6. Conclusion

We have presented a systematic method to determine the stability of discrete solitons in a \mathcal{PT} -symmetric coupler by computing the eigenvalues of the corresponding linear eigenvalue problem using asymptotic expansions. We have compared the analytical results that we obtained with numerical computations, where good agreement is obtained. From the numerics, we have also established the mechanism of instability as well as the stability region of the discrete solitons. The application of the method in higher dimensional \mathcal{PT} -symmetric couplers (see, e.g., [32]) is a natural

extension of the problem that is addressed for future work. Additionally, we also address the computation of eigenvalues of discrete solitons in the neighbourhood of broken \mathcal{PT} -symmetry as future investigations.

Appendix

Analytical Calculation

As mentioned in Section 4.2, to solve the eigenvalue problem (12) analytically we expand the eigenvalue and eigenvector asymptotically as

$$\square = \square^{(0)} + \sqrt{\epsilon}\square^{(1)} + \epsilon\square^{(2)} + \dots, \quad (\text{A.1})$$

with $\square = \lambda, K_n, L_n, P_n, Q_n$.

Performing the expansion in ϵ , at $\mathcal{O}(\epsilon^0)$, we obtain the following set of equations:

$$\lambda^{(0)} \underline{v}_n^{(0)} = \underbrace{\begin{bmatrix} \gamma & \omega - A_n^{(0)2} & 0 & -1 \\ 3(A_n^{(0)})^2 - \omega & \gamma & 1 & 0 \\ 0 & -1 & k_1 & k_2 \\ 1 & 0 & k_3 & -k_1 \end{bmatrix}}_{M_0} \underline{v}_n^{(0)}, \quad (\text{A.2})$$

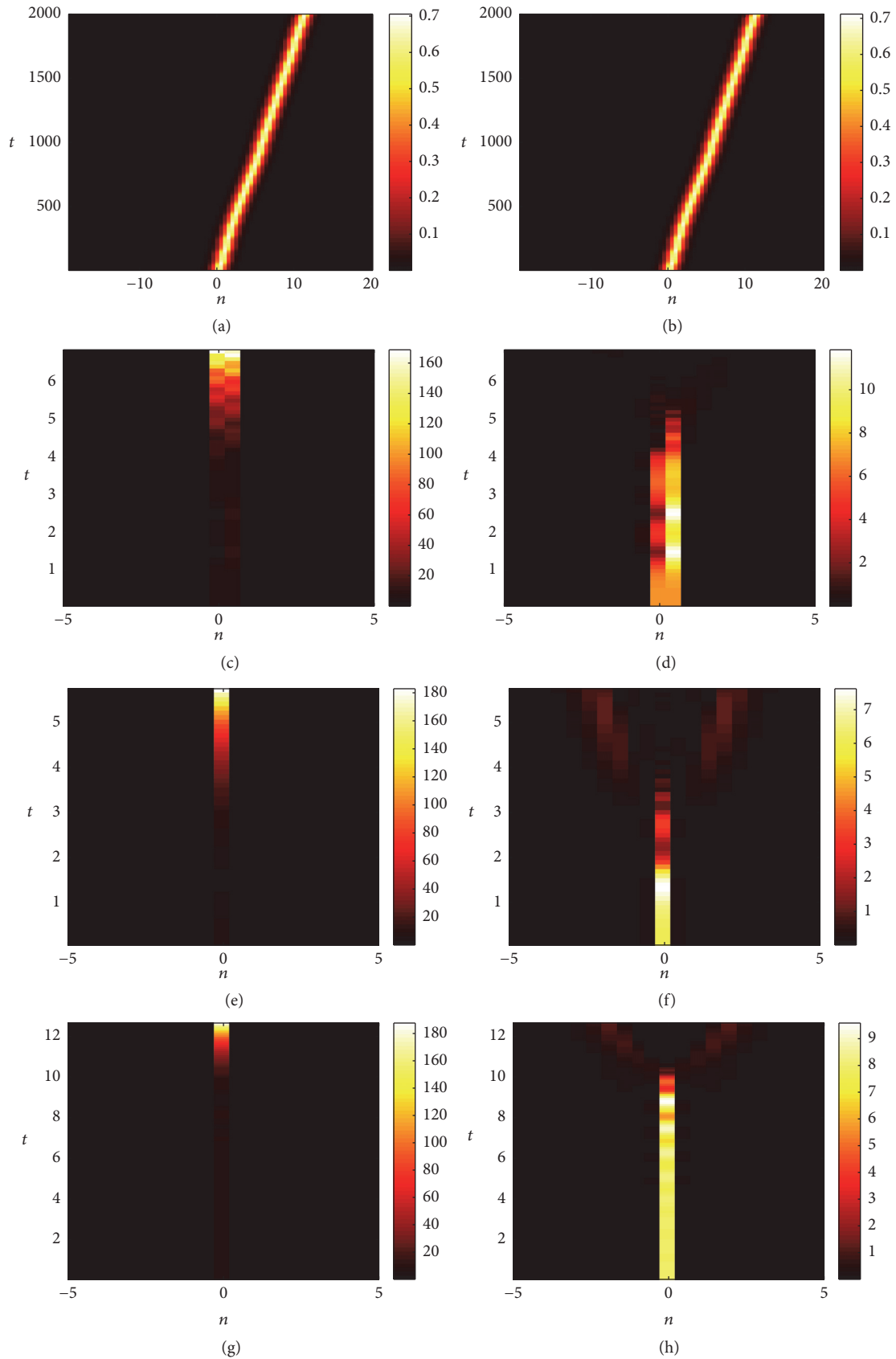


FIGURE 7: The typical dynamics of the instability of the discrete solitons in the previous figures. Here, $\gamma = 0.5$ and $\epsilon = 1$. Depicted in (a–h) are $|u_n|^2$ and $|v_n|^2$, respectively. (a–h) The dynamics of intersite soliton I with $\omega = 1.2$, intersite soliton II with $\omega = 5.2$, and onsite solitons I and II both with $\omega = 5.2$.

where

$$\underline{v}_n^{(j)} = \begin{bmatrix} K_n^{(j)} \\ L_n^{(j)} \\ P_n^{(j)} \\ Q_n^{(j)} \end{bmatrix}, \quad (A.3)$$

$$k_1 = -\left(2\Re(B_n^{(0)})\Im(B_n^{(0)}) + \gamma\right),$$

$$k_2 = \omega - \Re(B_n^{(0)})^2 - 3\Im(B_n^{(0)})^2,$$

$$k_3 = 3\Re(B_n^{(0)})^2 + \Im(B_n^{(0)})^2 - \omega.$$

At $\mathcal{O}(\epsilon^{1/2})$ and $\mathcal{O}(\epsilon^1)$, we obtain

$$\lambda^{(0)} \underline{v}_n^{(1)} = M_0 \underline{v}_n^{(2)} - \lambda^{(1)} \underline{v}_n^{(0)}, \quad (A.4)$$

$$\lambda^{(0)} M_0 = M_0 \underline{v}_n^{(2)} - \lambda^{(1)} \underline{v}_n^{(1)} - \lambda^{(2)} \underline{v}_n^{(0)}$$

$$+ \begin{bmatrix} 0 & 2(1 - A_n^{(0)} A_n^{(1)}) & 0 & 0 \\ 6A_n^{(0)} A_n^{(1)} - 2 & 0 & 0 & 0 \\ 0 & 0 & k_4 & 2 + k_5 \\ 0 & 0 & k_6 - 2 & -k_4 \end{bmatrix} \underline{v}_n^{(0)} \quad (A.5)$$

$$+ \begin{bmatrix} 0 & -1 & 0 & 0 \\ 1 & 0 & 0 & 0 \\ 0 & 0 & 0 & -1 \\ 0 & 0 & 1 & 0 \end{bmatrix} (\underline{v}_{n+1}^{(1)} + \underline{v}_{n-1}^{(1)}),$$

where

$$k_4 = -2\left(\Re(B_n^{(0)})\Im(B_n^{(1)}) + \Re(B_n^{(1)})\Im(B_n^{(0)})\right),$$

$$k_5 = -2\left(\Re(B_n^{(0)})\Re(B_n^{(1)}) + 3\Im(B_n^{(0)})\Im(B_n^{(1)})\right), \quad (A.6)$$

$$k_6 = 2\left(3\Re(B_n^{(0)})\Re(B_n^{(1)}) + \Im(B_n^{(0)})\Im(B_n^{(1)})\right).$$

The steps of finding the coefficients $\lambda^{(j)}$ of the asymptotic expansions, $j = 0, 1, 2, \dots$, are as follows:

- (i) Solve the eigenvalue problem (A.2), which is a 4×4 system of equations, for $\lambda^{(0)}$ and $\underline{v}_n^{(0)}$.
- (ii) Determine $\lambda^{(1)}$ by taking the vector inner product of both sides of (A.4) with the null-space of the Hermitian transpose of the block matrix that consists of $(M_0 - \lambda^{(0)} I_4)$ along the diagonal, where I_4 is the 4×4 identity matrix.
- (iii) Solve (A.4) for $\underline{v}_n^{(1)}$.
- (iv) Determine $\lambda^{(2)}$ by taking the vector inner product of both sides of (A.5) with the null-space of the Hermitian transpose of the block matrix that consists of $(M_0 - \lambda^{(0)} I_4)$.

The procedure repeats if one would like to calculate the higher order terms.

The leading order eigenvalue $\lambda^{(0)}$ of (A.2) has been solved in [31]. However, the expression of the corresponding eigenvector $\underline{v}_n^{(0)}$ was very lengthy, that makes it almost impractical to be used to determine the higher order corrections of $\lambda^{(j)}$. Therefore, in every equation at order $\mathcal{O}(\epsilon^\ell)$ obtained from (12), we also expand the variables in γ , that is,

$$M_j = M_{j,0} + \gamma M_{j,1} + \gamma^2 M_{j,2} = \dots, \quad (A.7)$$

$$\square^{(j)} = \square^{(j,0)} + \gamma \square^{(j,1)} + \gamma^2 \square^{(j,2)} + \dots,$$

where again $\square = \lambda, \underline{v}_n$, and obtain equations at order $\mathcal{O}(\gamma^{\tilde{\ell}})$. The steps to determine $\lambda^{(j,k)}$ and $\underline{v}_n^{(j,k)}$ are the same as mentioned above.

Competing Interests

The authors declare that there is no conflict of interests regarding the publication of this paper.

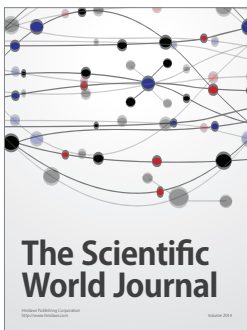
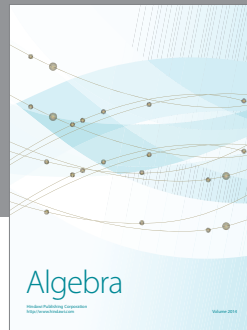
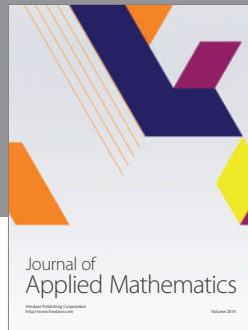
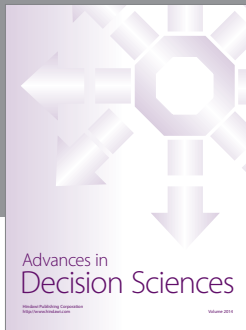
Acknowledgments

Alhaji A. Bachtiar and Hadi Susanto are grateful to the University of Nottingham for the 2013 Visiting Fellowship Scheme and British Council for the 2015 Indonesia Second City Partnership Travel Grant.

References

- [1] N. Moiseyev, *Non-Hermitian Quantum Mechanics*, Cambridge University Press, Cambridge, UK, 2011.
- [2] C. M. Bender and S. Boettcher, "Real spectra in non-hermitian hamiltonians having \mathcal{PT} symmetry," *Physical Review Letters*, vol. 80, no. 24, p. 5243, 1998.
- [3] C. M. Bender, S. Boettcher, and P. N. Meisinger, "PT-symmetric quantum mechanics," *Journal of Mathematical Physics*, vol. 40, no. 5, pp. 2201–2229, 1999.
- [4] C. M. Bender, "Making sense of non-Hermitian Hamiltonians," *Reports on Progress in Physics*, vol. 70, no. 6, p. 947, 2007.
- [5] A. Guo, G. J. Salamo, D. Duchesne et al., "Observation of PT-symmetry breaking in complex optical potentials," *Physical Review Letters*, vol. 103, no. 9, Article ID 093902, 2009.
- [6] C. E. Rüter, K. G. Makris, R. El-Ganainy, D. N. Christodoulides, M. Segev, and D. Kip, "Observation of parity-time symmetry in optics," *Nature Physics*, vol. 6, no. 3, pp. 192–195, 2010.
- [7] S. V. Suchkov, A. A. Sukhorukov, J. Huang, S. V. Dmitriev, C. Lee, and Yu. S. Kivshar, "Nonlinear switching and solitons in PT-symmetric photonic systems," *Laser & Photonics Reviews*, vol. 10, no. 2, pp. 177–213, 2016.
- [8] V. V. Konotop, J. Yang, and D. A. Zezyulin, "Nonlinear waves in \mathcal{PT} -symmetric systems," *Reviews of Modern Physics*, vol. 88, no. 3, Article ID 035002, 2016.
- [9] J. Pickton and H. Susanto, "Integrability of PT-symmetric dimers," *Physical Review A*, vol. 88, no. 6, Article ID 063840, 2013.
- [10] P. G. Kevrekidis, D. E. Pelinovsky, and D. Y. Tyugin, "Nonlinear dynamics in PT-symmetric lattices," *Journal of Physics. A. Mathematical and Theoretical*, vol. 46, no. 36, Article ID 365201, 2013.

- [11] I. V. Barashenkov, G. S. Jackson, and S. Flach, “Blow-up regimes in the \mathcal{PT} -symmetric coupler and the actively coupled dimer,” *Physical Review A*, vol. 88, no. 5, Article ID 053817, 2013.
- [12] S. V. Suchkov, B. A. Malomed, S. V. Dmitriev, and Y. S. Kivshar, “Solitons in a chain of parity-time-invariant dimers,” *Physical Review E*, vol. 84, no. 4, Article ID 046609, 2011.
- [13] P. L. Chu, B. A. Malomed, and G. D. Peng, “Soliton switching and propagation in nonlinear fiber couplers: analytical results,” *Journal of the Optical Society of America B*, vol. 10, no. 8, p. 1379, 1993.
- [14] E. M. Wright, G. I. Stegeman, and S. Wabnitz, “Solitary-wave decay and symmetry-breaking instabilities in two-mode fibers,” *Physical Review A*, vol. 40, no. 8, pp. 4455–4466, 1989.
- [15] N. Akhmediev and J. M. Soto-Crespo, “Propagation dynamics of ultrashort pulses in nonlinear fiber couplers,” *Physical Review E*, vol. 49, no. 5, pp. 4519–4529, 1994.
- [16] B. A. Malomed, I. M. Skinner, P. L. Chu, and G. D. Peng, “Symmetric and asymmetric solitons in twin-core nonlinear optical fibers,” *Physical Review E*, vol. 53, no. 4, pp. 4084–4091, 1996.
- [17] R. Driben and B. A. Malomed, “Stability of solitons in parity-time-symmetric couplers,” *Optics Letters*, vol. 36, no. 22, pp. 4323–4325, 2011.
- [18] F. K. Abdullaev, V. V. Konotop, M. Öggen, and M. P. Sørensen, “Zeno effect and switching of solitons in nonlinear couplers,” *Optics Letters*, vol. 36, no. 23, pp. 4566–4568, 2011.
- [19] R. Driben and B. A. Malomed, “Stabilization of solitons in PT models with supersymmetry by periodic management,” *EPL (Europhysics Letters)*, vol. 96, no. 5, Article ID 51001, 2011.
- [20] N. V. Alexeeva, I. V. Barashenkov, A. A. Sukhorukov, and Y. S. Kivshar, “Optical solitons in \mathcal{PT} -symmetric nonlinear couplers with gain and loss,” *Physical Review A*, vol. 85, no. 6, Article ID 063837, 2012.
- [21] I. V. Barashenkov, S. V. Suchkov, A. A. Sukhorukov, S. V. Dmitriev, and Y. S. Kivshar, “Breathers in \mathcal{PT} -symmetric optical couplers,” *Physical Review A*, vol. 86, no. 5, Article ID 053809, 2012.
- [22] P. Li, L. Li, and B. A. Malomed, “Multisoliton Newton’s cradles and supersolitons in regular and parity-time-symmetric nonlinear couplers,” *Physical Review E*, vol. 89, Article ID 062926, 2014.
- [23] J. D’Ambroise, P. G. Kevrekidis, and B. A. Malomed, “Staggered parity-time-symmetric ladders with cubic nonlinearity,” *Physical Review E*, vol. 91, no. 3, Article ID 033207, 11 pages, 2015.
- [24] G. Herring, P. G. Kevrekidis, B. A. Malomed, R. Carretero-González, and D. J. Frantzeskakis, “Symmetry breaking in linearly coupled dynamical lattices,” *Physical Review E. Statistical, Nonlinear, and Soft Matter Physics*, vol. 76, no. 6, Article ID 066606, 2007.
- [25] A. Chernyavsky and D. Pelinovsky, “Breathers in hamiltonian PT -symmetric chains of coupled pendula under a resonant periodic force,” *Symmetry*, vol. 8, no. 7, p. 59, 2016.
- [26] C. M. Bender, B. K. Berntson, D. Parker, and E. Samuel, “Observation of PT phase transition in a simple mechanical system,” *American Journal of Physics*, vol. 81, no. 3, pp. 173–179, 2013.
- [27] A. Chernyavsky and D. E. Pelinovsky, “Long-time stability of breathers in Hamiltonian \mathcal{PT} -symmetric lattices,” <https://arxiv.org/abs/1606.02333>.
- [28] R. S. MacKay and S. Aubry, “Proof of existence of breathers for time-reversible or Hamiltonian networks of weakly coupled oscillators,” *Nonlinearity*, vol. 7, no. 6, pp. 1623–1643, 1994.
- [29] V. V. Konotop, D. E. Pelinovsky, and D. A. Zezyulin, “Discrete solitons in PT-symmetric lattices,” *EPL*, vol. 100, no. 5, Article ID 56006, 2012.
- [30] D. E. Pelinovsky, D. A. Zezyulin, and V. V. Konotop, “Nonlinear modes in a generalized \mathcal{PT} -symmetric discrete nonlinear Schrödinger equation,” *Journal of Physics A: Mathematical and Theoretical*, vol. 47, no. 8, Article ID 085204, 2014.
- [31] K. Li and P. G. Kevrekidis, “ \mathcal{PT} -symmetric oligomers: analytical solutions, linear stability, and nonlinear dynamics-symmetric oligomers: analytical solutions, linear stability, and nonlinear dynamics,” *Physical Review E*, vol. 83, no. 6, Article ID 066608, 2011.
- [32] Z. Chen, J. Liu, S. Fu, Y. Li, and B. A. Malomed, “Discrete solitons and vortices on two-dimensional lattices of PT-symmetric couplers,” *Optics Express*, vol. 22, no. 24, pp. 29679–29692, 2014.



Hindawi

Submit your manuscripts at
<http://www.hindawi.com>

